# Propagation dynamics of controlled cross-talk via interplay between $\chi^{(1)}$ and $\chi^{(3)}$ processes

Paul S. Hsu,[1,2,*] George R. Welch,[2] James R. Gord,[3] and Anil K. Patnaik[3,4]
[1]*Spectral Energies, LLC, 5100 Springfield Street, Suite 301, Dayton, Ohio 45431, USA*
[2]*Institute for Quantum Studies and Department of Physics, Texas A&M University, College Station, Texas 77843, USA*
[3]*Air Force Research Laboratory, Propulsion Directorate, Wright-Patterson AFB, Ohio 45433, USA*
[4]*Department of Physics, Wright State University, Dayton, Ohio 45435, USA*
(Received 15 February 2011; published 12 May 2011)

We investigate theoretically and experimentally the propagation dynamics of a nonlinear cross-talk effect between two probe channels in a double-ladder system and show that an interplay between $\chi^{(1)}$ and $\chi^{(3)}$ processes leads to the control of cross-talk. We derive analytical solutions to describe the propagation dynamics of the probe fields with the cross-talk effect built in. From the analytical results we identify and examine the regimes of interest where contributions of either $\chi^{(1)}$ or $\chi^{(3)}$ or both are significant. The control of cross-talk is demonstrated experimentally, and good quantitative agreement is found between the analytical solutions and the experiment.

DOI: 10.1103/PhysRevA.83.053819 PACS number(s): 42.50.Gy, 32.80.−t, 42.65.Hw, 42.25.Bs

## I. INTRODUCTION

Nonlinear optical processes in light-matter interactions can be greatly enhanced and controlled via resonant processes such as electromagnetically induced transparency (EIT) [1–4]. In a typical three-level ladder-type EIT system, the optical response of the medium to a weak probe field is determined by the atomic susceptibility $\chi^{(1)}$ to the first order in the probe field, which is manipulated by a control laser field [5]. With an additional control field coupling to a fourth atomic level, the $\chi^{(3)}$ process can significantly affect the dispersion [6] and absorption [7,8] properties of the probe field. The efficient parametric generation of a four wave-mixing (FWM) field using the resonant $\chi^{(3)}$ process in a four-level double-ladder atomic system has been recently demonstrated [6,8–14]. In particular, this system allows efficient frequency up-conversion [10–12] and down-conversion [13,14] through the use of low-power continuous-wave lasers that can be used for ultraviolet generation and quantum communication [11–14]. Previous experimental and theoretical studies of the double-ladder system have also revealed many remarkable properties that are sensitive to the phase and amplitude of the control laser and can be used for polarization control and laser-frequency stabilization [15–23]. Wielandy and Gaeta demonstrated the use of quantum coherence to control the polarization state of the probe field [15]. They reported large birefringence and hence large polarization rotation for generating any arbitrary polarization state of a laser beam. Patnaik and Agarwal theoretically showed that the polarization state of the probe can be dynamically controlled using a static magnetic field in conjunction with control laser fields in both homogeneously [16] and inhomogeneously [17] broadened double-ladder media. Several experimental and theoretical studies have been demonstrated recently on large laser-induced birefringence and magneto-optical rotation in ytterbium and cesium atoms [18–21]. Morigi and co-workers theoretically showed that a double-ladder system (which is termed a closed-loop diamond configuration) allows one to control the optical properties of the medium using the phase of the laser fields [22,23]. Similar phase-sensitive control has been experimentally demonstrated in a closed double-$\Lambda$ system using sodium atom [24,25].

Recently, we have experimentally demonstrated the efficient generation of a FWM field in the double-ladder system via the resonant $\chi^{(3)}$ process [8,9]. In our theoretical studies, we showed that with two control fields in such systems, the medium polarization of each probe transition is dominated by both $\chi^{(1)}$ and $\chi^{(3)}$ processes [8]. However, the propagation effects dominated by a strong cross-talk between the two probe channels have never been discussed in the literature. In an earlier theoretical study, Menon and Agarwal have reported gain and weak transparency due to cross-talk between optical transitions in a driven $\Lambda$ system, where both the probe and drive fields couple to the same transition [26]. They considered a thin medium and used dressed-state analysis to demonstrate the rich interference effects in absorption spectra of the system. In this paper, we present analytical solutions for the propagation dynamics of two probe fields coupled to the double-ladder configuration taking the cross-talk effect into account and also experimentally demonstrate control of the cross-talk.

The outline of this paper is as follows: We describe the system and present the corresponding dynamical equation in Sec. II. In Sec. III we derive the analytical solutions for describing the dynamics of propagation of the probe fields in the double-ladder atomic system, and show that the behavior of the probe field during propagation in the medium is strongly affected by the interplay of the $\chi^{(1)}$ and $\chi^{(3)}$ processes. In Sec. IV we experimentally demonstrate the control of cross-talk and show that the experimental results and the theoretical calculations are in good quantitative agreement. In Sec. V, we conclude with a summary of the results.

## II. ATOMIC DYNAMICS

In this section we present a theoretical formulation that describes the dynamics of a double-ladder atomic system (shown in Fig. 1) and investigate the effect of cross-talk on the susceptibility of the medium. We consider the cascaded transitions $|b\rangle(|j=0,m_j=0\rangle)\longleftrightarrow|i\rangle(|j=1,m_j=\pm1\rangle)\longleftrightarrow|c\rangle(|j=0,m_j=0\rangle)$ $(i=a,a')$. Here $|a\rangle$ and $|a'\rangle$ are magnetic sublevels with $m_j=\pm1$. A linearly polarized

*paul.hsu@wpafb.af.mil

 

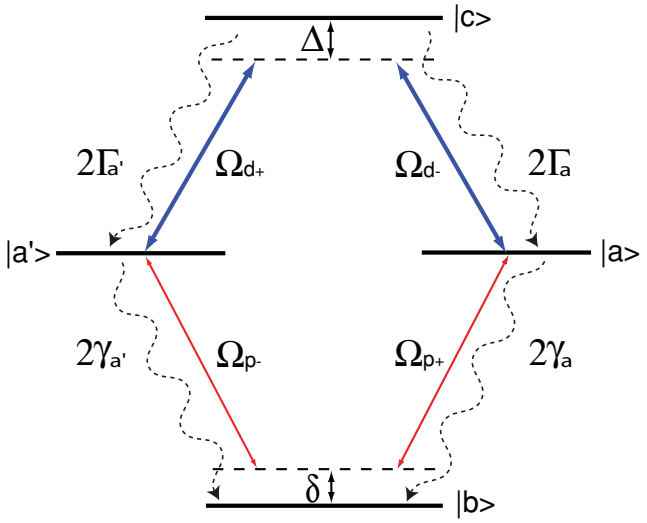


FIG. 1. (Color online) Energy-level diagram of the double-ladder system under consideration. Here $2\Gamma_i$ ($2\gamma_i$) is the radiative decay of the drive (probe) transition ($i = a,a'$), and $\Omega_{d\pm}$ ($\Omega_{p\pm}$) and $\Delta$ ($\delta$) are the Rabi frequency and the frequency detuning of the drive (probe) field, respectively. The intermediate states $|a\rangle$ and $|a'\rangle$ correspond to Zeeman sublevels with $m_j = \pm 1$.

weak probe field $E_p$ couples the transitions $|b\rangle$ to $|a\rangle$ and $|a'\rangle$, while a strong drive field $E_d$ couples $|a\rangle$ and $|a'\rangle$ to $|c\rangle$. Considering the circular component of each field, we have four monochromatic fields coupling to their corresponding polarization channels; e.g., $E_{p+}$ ($E_{p-}$) couples $|b\rangle \longleftrightarrow |a\rangle$ ($|b\rangle \longleftrightarrow |a'\rangle$) and $E_{d+}$ ($E_{d-}$) couples $|a'\rangle \longleftrightarrow |c\rangle$ ($|a\rangle \longleftrightarrow |c\rangle$) transitions.

The equation of motion for the double-ladder system is given by the density-matrix equation as [17]

$$\begin{aligned}\frac{\partial\rho}{\partial t} &= \frac{-i}{\hbar}[\mathcal{H}_o + \mathcal{H}_I, \rho] \\ &\quad - \sum_{i=a,a'} (\Gamma_i\{|c\rangle\langle c|,\rho\}_+ + \gamma_i\{|i\rangle\langle i|,\rho\}_+ \\ &\quad - 2\Gamma_i\rho_{cc}|i\rangle\langle i| - 2\gamma_i\rho_{ii}|b\rangle\langle b|). \end{aligned} \tag{1}$$

Note that the decay coefficients are inserted phenomenologically. The radiative decay rates for the drive and probe transition are $2\Gamma_i$ and $2\gamma_i$ (with $i = a,a'$), respectively. The curly brackets $\{\}_+$ are anticommutators of the operators.

To eliminate the rapid temporal oscillations in the density-matrix equation, we use the following transformation $\rho \to \tilde{\rho}$ with elements given by

$$\begin{aligned} \rho_{jb} &= \tilde{\rho}_{jb}e^{-iw_pt}, \quad \rho_{cj} = \tilde{\rho}_{cj}e^{-iw_dt}, \\ \rho_{cb} &= \tilde{\rho}_{cb}e^{-i(w_p+w_d)t}, \quad \rho_{j'j'} = \tilde{\rho}_{j'j'}, \end{aligned} \tag{2}$$

where $j = a,a'$ and $j' = j,b,c$. Here, $w_p$ ($w_d$) represents the central frequency of the probe (drive) laser field. Then, the matrix equation for $\tilde{\rho}$ can be rewritten as

$$\begin{aligned}\dot{\tilde{\rho}}_{\alpha\beta} &= \frac{-i}{\hbar}\langle\alpha|[\mathcal{H}_{\rm eff},\tilde{\rho}]|\beta\rangle \\ &\quad - \sum_{i=a,a'} \langle\alpha|[\Gamma_i\{|c\rangle\langle c|,\tilde{\rho}\}_+ + \gamma_i\{|i\rangle\langle i|,\tilde{\rho}\}_+ \\ &\quad - 2\Gamma_i\tilde{\rho}_{cc}|i\rangle\langle i| - 2\gamma_i\tilde{\rho}_{ii}|b\rangle\langle b|]|\beta\rangle, \end{aligned} \tag{3}$$

with the effective Hamiltonian in the transformed frame

$$\begin{aligned}\mathcal{H}_{\rm eff} &= \hbar(\delta+\Delta)|c\rangle\langle c| + \hbar\delta(|a\rangle\langle a| + |a'\rangle\langle a'|) \\ &\quad - \hbar(\Omega_{p+}|a\rangle\langle b| + \Omega_{p-}|a'\rangle\langle b| \\ &\quad + \Omega_{d-}|c\rangle\langle a| + \Omega_{d+}|c\rangle\langle a'| + \text{H.c.}). \end{aligned} \tag{4}$$

Here, $\delta$ ($\Delta$) and $\Omega_{p\pm}$ ($\Omega_{d\pm}$) are the frequency detunings and the coupling Rabi frequencies of the probe (drive) field, respectively. For simplicity $\Gamma_i = \Gamma$ and $\gamma_i = \gamma$ are assumed in the following calculations. Please note that the tilde sign in $\tilde{\rho}$ has been removed in the following for the sake of brevity.

Next, the complex susceptibility at the probe frequency is obtained from the atomic polarization $\mathcal{P}_\pm = N\wp_p\rho_\pm$. Here $\rho_\pm$ is the density-matrix element corresponding to the probe transition ($\rho_+ \equiv \rho_{ab}$, $\rho_- \equiv \rho_{a'b}$), $\wp_p$ is the reduced dipole matrix element involved in the probe transition, and $N$ is the atomic density. To obtain the atomic polarization $\mathcal{P}_\pm$ created by atomic coherence in the probe transition, we calculate the steady-state solutions of the off-diagonal coherence terms $\rho_{ab}$ and $\rho_{a'b}$. Assuming $|\Omega_{d\pm}| \gg |\Omega_{p\pm}|$, the analytical solutions for the coherences are calculated to the first order in both weak fields $\Omega_{p+}$ and $\Omega_{p-}$ by solving Eq. (3). The coherence matrix elements are obtained as

$$\rho_{ab} = \Lambda^{(1)}_{ab}\Omega_{p+} + \Lambda^{(3)}_{ab}\Omega_{p-}, \tag{5}$$

$$\rho_{a'b} = \Lambda^{(1)}_{a'b}\Omega_{p-} + \Lambda^{(3)}_{a'b}\Omega_{p+}, \tag{6}$$

where

$$\begin{aligned}\Lambda^{(1)}_{ab} &= \frac{i\{|\Omega_{d+}|^2 + (\gamma+i\delta)[2\Gamma + i(\Delta+\delta)]\}}{D}, \\ \Lambda^{(3)}_{ab} &= \frac{-i\Omega^*_{d-}\Omega_{d+}}{D}, \\ \Lambda^{(1)}_{a'b} &= \frac{i\{|\Omega_{d-}|^2 + (\gamma+i\delta)[2\Gamma + i(\Delta+\delta)]\}}{D}, \\ \Lambda^{(3)}_{a'b} &= \frac{-i\Omega_{d-}\Omega^*_{d+}}{D}, \end{aligned}$$

and

$$D = \{|\Omega_{d+}|^2 + |\Omega_{d-}|^2 + (\gamma+i\delta)[2\Gamma + i(\Delta+\delta)]\}(\gamma+i\delta). \tag{7}$$

The above solutions (5) and (6) are special cases of the solutions obtained in Ref. [8] in the absence of the magnetic field. As summarized in Ref. [8], the atomic polarizations $\mathcal{P}_{ab}$ and $\mathcal{P}_{a'b}$ are linear combinations of the $\chi^{(1)}$ and $\chi^{(3)}$ processes. Here $\Lambda^{(1)}_{ab}$ corresponds to the first-order contribution from the weak probe $\Omega_{p+}$ in the transition $|a\rangle \longleftrightarrow |b\rangle$. The second term $\Lambda^{(3)}_{ab}$ in $\rho_{ab}$ depicts the three-photon process via the absorption of $\Omega_{p-}$ and $\Omega_{d+}$, followed by stimulated emission in $\Omega_{d-}$ that results in a nonzero third-order contribution to the atomic coherence. A similar explanation can be used for $\Lambda^{(1)}_{a'b}$ and $\Lambda^{(3)}_{a'b}$ in $\rho_{a'b}$.

This paper has distinctly different goals and physics compared to Ref. [8]. (a) Even though both probe fields $\Omega_{p\pm}$ are taken into account in the calculation in Ref. [8], there the theoretical analysis was focused on generation of a $\chi^{(3)}$ field in the presence of only one probe field in the double-ladder system. In this paper, we investigate the effect of interplay of $\chi^{(1)}$ and $\chi^{(3)}$ processes on both the probe transitions when both

the probe fields are simultaneously coupled. (b) The resonant three-photon processes $\Lambda^{(3)}_{ab}$ and $\Lambda^{(3)}_{a'b}$ can efficiently transfer energy between the two probe transitions, which establish the cross-talk between the two probe channels. The cross-talk and hence the probe behaviors are strongly affected by the interplay of the $\chi^{(1)}$ and $\chi^{(3)}$ processes during the propagation of the fields inside the medium. The corresponding probe field propagation dynamics will be discussed in the following section. Note that these dynamical solutions are valid for denser medium, which is in contrast to Ref. [8], where the calculated susceptibilities $\chi^{(1)}$ and $\chi^{(3)}$ were good only for low-density thin cell or few atoms cases.

## III. CONTROLLED PROPAGATION DYNAMICS OF CROSS-TALK

The propagation dynamics of the probe fields along the $z$ direction in the medium that explicitly include the cross-talk effect are obtained by solving the Maxwell-Bloch equation [27]

$$\begin{aligned}\frac{\partial \Omega_{p\pm}}{\partial z} &= -\frac{k_p \wp_p}{2\epsilon_0 \hbar}\mathrm{Im}[\mathcal{P}_\pm] \\ &= -\eta \mathrm{Im}[\rho_\pm],\end{aligned} \tag{8}$$

where $k_p$ corresponds to the propagation constant of the probe field, and $\eta = k_p {\wp_p}^2 N/2\hbar\epsilon_0$ is a constant obtained from system parameters that is proportional to the inverse of the optical depth. Using the analytical solutions (5) and (6), the Maxwell-Bloch equations (8) can be expressed in matrix form as

$$\frac{\partial}{\partial z}\begin{pmatrix}\Omega_{p+}(z)\\ \Omega_{p-}(z)\end{pmatrix} = i\eta\begin{pmatrix}\Lambda^{(1)}_{ab} & \Lambda^{(3)}_{ab}\\ \Lambda^{(3)}_{a'b} & \Lambda^{(1)}_{a'b}\end{pmatrix}\begin{pmatrix}\Omega_{p+}(z)\\ \Omega_{p-}(z)\end{pmatrix}. \tag{9}$$

The $2\times 2$ matrix is a *cross-talk matrix* that describes the interplay between the $\chi^{(1)}$ and $\chi^{(3)}$ processes. In the absence of any one of the drive fields $\Omega_{d\pm}$, $\Lambda^{(3)}_{\alpha\beta}=0$, and hence no cross-talk occurs between the two probe channels. The probe field dynamics are calculated by obtaining the eigenvalues and eigenfunctions of the cross-talk matrix. Thus, the solution for $\Omega_{p\pm}$ obtained from solving Eq. (9) is

$$\begin{pmatrix}\Omega_{p+}(z)\\ \Omega_{p-}(z)\end{pmatrix} = C_+ e^{-(\alpha_{LT})\eta z}\begin{pmatrix}\Omega^*_{d-}\\ \Omega^*_{d+}\end{pmatrix} + C_- e^{-(\alpha_{2L})\eta z}\begin{pmatrix}-\Omega_{d+}\\ \Omega_{d-}\end{pmatrix}, \tag{10}$$

where $\alpha_{LT}$ is the susceptibility dominated by terms that describe the transparency in a ladder system, $\alpha_{2L}$ corresponds to the susceptibility of a two-level system, and $C_\pm$ is a constant that is obtained from input field parameters. They are given by

$$\begin{aligned}\alpha_{LT} &= \frac{2\Gamma + i(\Delta+\delta)}{|\Omega_{d+}|^2 + |\Omega_{d-}|^2 + (\gamma+i\delta)[2\Gamma + i(\Delta+\delta)]},\\ \alpha_{2L} &= \frac{1}{\gamma + i\delta},\\ C_+ &= \frac{\Omega_{p-}(0)\Omega_{d+} + \Omega_{p+}(0)\Omega_{d-}}{|\Omega_{d+}|^2 + |\Omega_{d-}|^2},\\ C_- &= \frac{\Omega_{p-}(0)\Omega^*_{d-} - \Omega_{p+}(0)\Omega^*_{d+}}{|\Omega_{d+}|^2 + |\Omega_{d-}|^2}.\end{aligned} \tag{11}$$

Note that these solutions are obtained assuming $\Omega_{d\pm}$ remains unchanged during propagation through the medium; $\Omega_{d\pm}(z=0) = \Omega_{d\pm}(z=l)$, where $l$ is the length of the medium. The solutions derived for the evolution of the probe $\sigma_{p+}$ and $\sigma_{p-}$ fields along the $z$ direction in the medium can be written explicitly as

$$\begin{aligned}\Omega_{p+}(z) = &\underbrace{\frac{\Omega_{p+}(0)|\Omega_{d-}|^2 + \Omega_{p-}(0)\Omega_{d+}\Omega^*_{d-}}{|\Omega_{d+}|^2 + |\Omega_{d-}|^2} e^{-(\alpha_{LT})\eta z}}_{\text{Ladder Transparency}}\\ &+ \underbrace{\frac{\Omega_{p+}(0)|\Omega_{d+}|^2 - \Omega_{p-}(0)\Omega_{d+}\Omega^*_{d-}}{|\Omega_{d+}|^2 + |\Omega_{d-}|^2} e^{-(\alpha_{2L})\eta z}}_{\text{Two-Level Absorption}},\end{aligned} \tag{12}$$

$$\begin{aligned}\Omega_{p-}(z) = &\frac{\Omega_{p-}(0)|\Omega_{d+}|^2 + \Omega_{p+}(0)\Omega_{d-}\Omega^*_{d+}}{|\Omega_{d+}|^2 + |\Omega_{d-}|^2} e^{-(\alpha_{LT})\eta z}\\ &+ \frac{\Omega_{p-}(0)|\Omega_{d-}|^2 - \Omega_{p+}(0)\Omega_{d-}\Omega^*_{d+}}{|\Omega_{d+}|^2 + |\Omega_{d-}|^2} e^{-(\alpha_{2L})\eta z}.\end{aligned} \tag{13}$$

Note that the first terms in both Eqs. (12) and (13) represent the transparency experienced by $\Omega_{p\pm}$ due to two drive fields $\Omega_{d\pm}$. The solution has a form equivalent to the transparency in a ladder system but with a modification due to the presence of a second drive field. The second terms in both equations represent absorption in two-level systems, but the amplitude is being modified by the amplitudes of the input fields.

To separate specifically the $\chi^{(1)}$ and $\chi^{(3)}$ contributions to $\Omega_{p\pm}$, we rewrite the expression for $\Omega_{p+}(z)$ as

$$\begin{aligned}\Omega_{p+}(z) = &\underbrace{\Omega_{p+}(0)\left(\frac{|\Omega_{d-}|^2 e^{-(\alpha_{LT})\eta z} + |\Omega_{d+}|^2 e^{-(\alpha_{2L})\eta z}}{|\Omega_{d+}|^2 + |\Omega_{d-}|^2}\right)}_{\chi^{(1)}\text{ contribution}}\\ &+ \underbrace{\Omega_{p-}(0)\Omega_{d+}\Omega^*_{d-}\left(\frac{e^{-(\alpha_{LT})\eta z} - e^{-(\alpha_{2L})\eta z}}{|\Omega_{d+}|^2 + |\Omega_{d-}|^2}\right)}_{\chi^{(3)}\text{ contribution}}.\end{aligned} \tag{14}$$

A similar expression is obtained for $\Omega_{p-}(z)$. The $\chi^{(3)}$ term in Eq. (14) represents the cross-talk control term. Clearly, the cross-talk between the two components of the probe field $\Omega_{p\pm}(z)$ can be controlled via the amplitude ($\Omega_{d\pm}$) as well as the phase of the two drive fields (considering the complex Rabi frequencies $\Omega_\alpha\Omega^*_\beta$) as shown in Eq. (14).

To extract the physical meaning from the above equations, we analyze Eqs. (12) and (13) for the following conditions : (i) When only the weak probe field $\Omega_{p+}$ and the strong drive field $\Omega_{d-}$ are present [and $\Omega_{p-}(0) = \Omega_{d+} = 0$] and both are on resonance with their respective transitions, the probe experiences increased transmission through the medium around $\delta = 0$ because of the EIT experienced by $\Omega_{p+}$ in the ladder configuration as shown in Fig. 2(a). The increased transmission of the probe field can be understood because of the creation of the dark state between the states $|c\rangle$ and $|b\rangle$. This result can be seen directly from our analytical solution

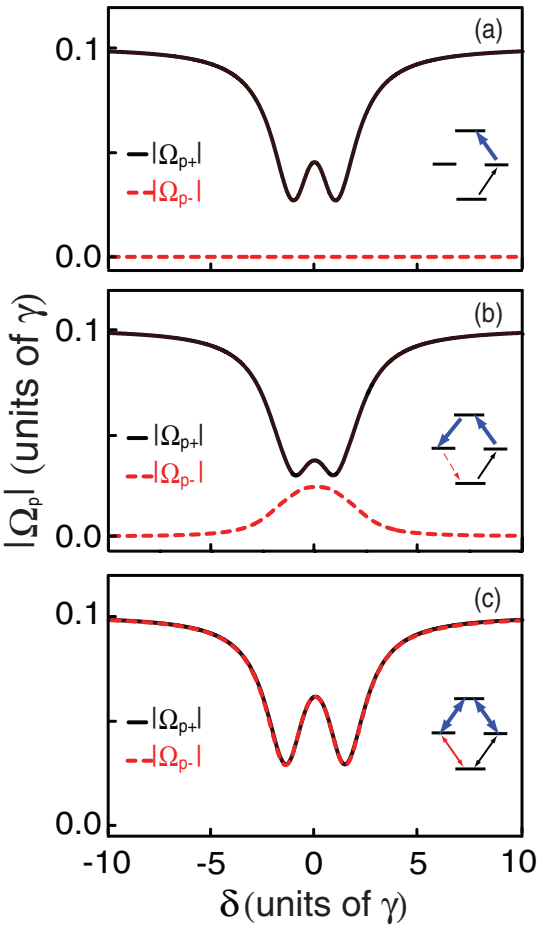


FIG. 2. (Color online) Rabi frequency of the probe field at the exit of the medium as a function of probe detuning from resonance under various conditions. The solid lines represent probe $|\Omega_{p+}|$, and the dashed lines represent probe $|\Omega_{p-}|$, with $\Delta = 0, \Gamma = 0.3$, and $\eta z = 2$. (a) $\Omega_{p+}(0) = 0.1$, $\Omega_{d-} = 1$, $\Omega_{p-}(0) = \Omega_{d+} = 0$; (b) $\Omega_{p+}(0) = 0.1$, $\Omega_{d-} = \Omega_{d+} = 1$, $\Omega_{p-}(0) = 0$; (c) $\Omega_{p+}(0) = \Omega_{p-}(0) = 0.1$, $\Omega_{d-} = \Omega_{d+} = 1$. All frequencies are scaled with $\gamma$.

by dropping the *two-level absorption* term from Eq. (12), such that only the *ladder-transparency* term

$$\Omega_{p+}(z) = \Omega_{p+}(0)\exp\left[\frac{-[2\Gamma + i(\Delta+\delta)]\eta z}{|\Omega_{d-}|^2 + (\gamma + i\delta)[2\Gamma + i(\Delta+\delta)]}\right] \tag{15}$$

survives. Furthermore, if we let $\Omega_{d-} = \Omega_{p-}(0) = 0$ and $\Omega_{d+} \neq 0$, Eq. (12) reduces to

$$\Omega_{p+}(z) = \Omega_{p+}(0)\exp\left[\frac{-\eta z}{\gamma + i\delta}\right], \tag{16}$$

which is a typical solution for a field propagating inside a two-level system.

(ii) If the strong resonant drive field $\Omega_{d+}$ is applied to the ladder-EIT configuration in addition to $\Omega_{d-}$ while maintaining $\Omega_{p-}(0) = 0$ [as shown in the inset of Fig. 2(b)], then the dark state created by $\Omega_{p+}$ and $\Omega_{d-}$ is perturbed, increasing the absorption of the probe $\Omega_{p+}$. The absorption of $\Omega_{p+}$ followed by $\Omega_{d-}$ optically pumps the population to state $|c\rangle$, which is then coherently transferred to state $|a'\rangle$ via the $\Omega_{d+}$ field; this generates third-order polarization $\rho_{a'b}$ and hence $\Omega_{p-}$ field, shown as a dashed line in Fig. 2(b). If the optical depth is large for $\Omega_{p-}$, then the generated $\Omega_{p-}$ field can also be absorbed along the $z$ direction during propagation. This leads to a gain in $\Omega_{p+}$ field due to the three-photon process $(\Omega_{p-}\Omega_{d+}\Omega_{d-}^*)$ via the transition $|b\rangle \to |a'\rangle \to |c\rangle \to |a\rangle$, which causes the cross-talk between the two probe channels. For long propagation distances, the amplitude and width of the spectra for both the generated field and the probe field are similar around $\delta = 0$.

(iii) Next, we consider the case where all four fields ($\Omega_{p\pm}$ and $\Omega_{d\pm}$) are present. Let us consider the case where the amplitudes of the drive fields are the same $[\Omega_{d+} = \Omega_{d-} = \Omega_d]$, the amplitudes of the input probe fields also are the same $[\Omega_{p+}(0) = \Omega_{p-}(0) = \Omega_p(0)]$, all of the drive fields are resonant with their respective transitions ($\Delta = 0$), and all of the probe fields have the same detuning. Under such conditions the transmission spectra for the two probe fields are identical because of the symmetric configuration of the double-ladder system, shown in Fig. 2(c). Equations (12) and (13) for the probe field can be reduced to

$$\Omega_{p+}(z) = \Omega_p(0)\exp\left[\frac{-(2\Gamma + i\delta)\eta z}{2|\Omega_d|^2 + (\gamma + i\delta)(2\Gamma + i\delta)}\right] = \Omega_{p-}(z). \tag{17}$$

The width of the transmission spectra of the two probe fields is broader than those of the ladder-EIT configuration as shown in Fig. 2(a). It should further be noted that the amplitude of the probe transmission of $\Omega_{p+}$ is higher than that in the regular ladder-EIT. This may be understood as follows: With the established dual-ladder coherences in the two probe transitions, the dark state (the antisymmetric state of $|c\rangle$ and $|b\rangle$) is more robust with the symmetric configuration in the double-ladder system. Details of the enhancement in probe transmission will be discussed elsewhere. The increase in transmission linewidth could be due to power broadening by the two strong drive fields.

In (iii) we studied the case of symmetric configuration in the double-ladder system, where the two probes are symmetric and the two drives are symmetric $[\Omega_{p-}(0) = \Omega_{p+}(0), \Omega_{d-} = \Omega_{d+}]$. In the following we consider the cases of asymmetric probe and drive amplitudes in the system where all of the fields are present with either the probe fields being asymmetric $[\Omega_{p-}(0) \neq \Omega_{p+}(0), \Omega_{d-} = \Omega_{d+}]$ or the drive fields being asymmetric $[\Omega_{d-} \neq \Omega_{d+}, \Omega_{p-}(0) = \Omega_{p+}(0)]$ or both the probe and drive fields being asymmetric $[\Omega_{p-}(0) \neq \Omega_{p+}(0), \Omega_{d-} \neq \Omega_{d+}]$. Here, all of the drive fields are resonant with their respective transitions $\Delta = 0$, and all of the probe fields have the same frequency detunings. Furthermore, the dynamics of probe propagation in the double-ladder media for the three cases above are discussed to bring out the clear physics of controlled cross-talk.

(iv) Let us first discuss the case of probe asymmetry and drive symmetry $[\Omega_{p-}(0) = 2\Omega_{p+}(0), \Omega_{d-} = \Omega_{d+}]$. In Fig. 3(a), we present the probe fields $\Omega_{p\pm}$ at the exit of the medium as a function of their detunings for three different propagation distances. For $\eta z = 2\gamma$, at $\delta = 0$ in

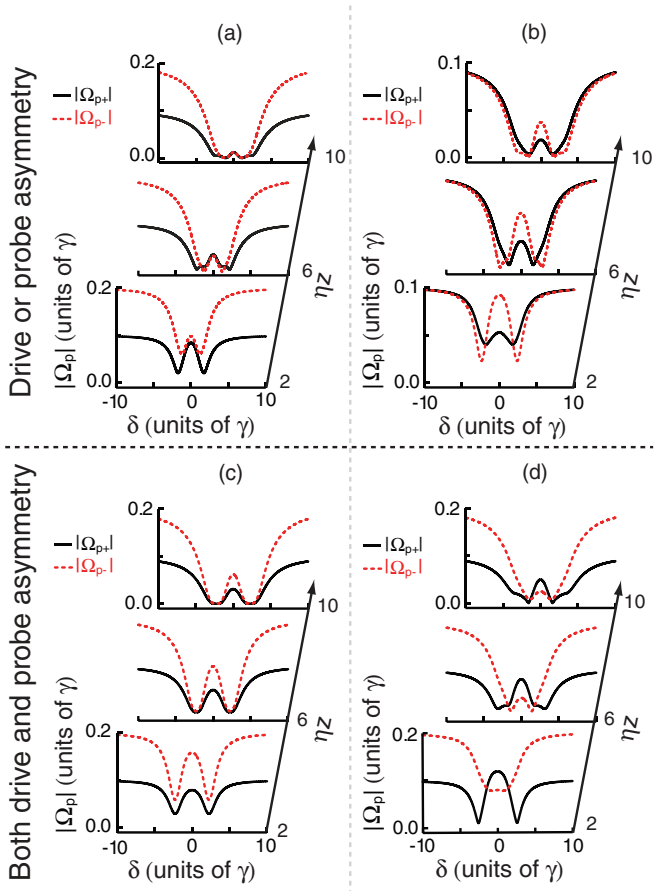


FIG. 3. (Color online) Rabi frequency of the probe field at different propagation distances $\eta z$ and as a function of probe detuning $\delta$ around resonance under various asymmetric field conditions. The solid lines represent probe $|\Omega_{p+}|$, and the dashed lines represent probe $|\Omega_{p-}|$ with $\Delta = 0$ and $\Gamma = 0.3$. Probe asymmetric case: (a) $\Omega_{p+}(0) = 0.1$, $\Omega_{p-}(0) = 0.2$, $\Omega_{d-} = \Omega_{d+} = 1$. Drive asymmetric case: (b) $\Omega_{p+}(0) = \Omega_{p-}(0) = 0.1$, $\Omega_{d-} = 1$, $\Omega_{d+} = 2$. Both probe and drive asymmetric cases: (c) $\Omega_{p+}(0) = 0.1$, $\Omega_{p-}(0) = 0.2$, $\Omega_{d-} = 1$, $\Omega_{d+} = 2$. Same as (c) but with $\Omega_{d\pm}$ intensities reversed: (d) $\Omega_{p+}(0) = 0.1$, $\Omega_{p-}(0) = 0.2$, $\Omega_{d-} = 2$, $\Omega_{d+} = 1$. All frequencies are scaled with $\gamma$.

addition to the transparency of $\Omega_{p+}$, it is clear that a gain occurs in $\Omega_{p+}$ because of the cross-talk via the third-order process $(\Omega_{p-}\Omega_{d+}\Omega_{d-}^{*})$ that is associated with a net loss of $\Omega_{p-}$. For a longer medium length ($\eta z = 6\gamma$ or $10\gamma$), the residual absorption of both the probes at $\delta = 0$ reduces the transmission of $\Omega_{p\pm}$ fields. Also, for a longer medium length, the transmission spectra of both the probes are similar around $\delta = 0$ because the resonant energy transfer between the two probe fields equilibrates along the medium length via cross-talk. This effect becomes insignificant for off-resonant probes.

(v) Next, we consider the case where the probes are symmetric $[\Omega_{p-}(0) = \Omega_{p+}(0)]$ and the two drives are asymmetric $(\Omega_{d+} = 2\Omega_{d-})$. Under such conditions the transmission of $\Omega_{p-}$ is higher than that of $\Omega_{p+}$ around $\delta = 0$ because of a stronger ladder transparency created by the strong drive $\Omega_{d+}$ field, as shown in Fig. 3(b). Even though the strengths of the probe fields are the same, the stronger ladder transparency of $\Omega_{p-}$ is maintained along the length of the medium such that $\Omega_{p-}(z) > \Omega_{p+}(z)$.

(vi) For both drive and probe being asymmetric fields $[\Omega_{p-}(0) \neq \Omega_{p+}(0), \Omega_{d-} \neq \Omega_{d+}]$, let us consider two cases where (a) a weak (strong) drive field couples to the corresponding weak (strong) probe field $(\Omega_{p-}(0) = 2\Omega_{p+}(0), \Omega_{d+} = 2\Omega_{d-})$ and (b) a strong (weak) drive field couples to the corresponding weak (strong) probe field $[\Omega_{p-}(0) = 2\Omega_{p+}(0), \Omega_{d-} = 2\Omega_{d+}]$. In case (a) both the probe $\Omega_{p+}$ and $\Omega_{p-}$ fields show high transmission throughout the medium because of the strong EIT created by the drive $\Omega_{d-}$ and $\Omega_{d+}$ in the $\sigma_{p+}$ and $\sigma_{p-}$ transitions, respectively [see Fig. 3(c)]. In case (b) the transmission of $\Omega_{p+}$ is higher than that of $\Omega_{p-}$ around $\delta = 0$ even though the initial $\Omega_{p-}(0)$ is greater than $\Omega_{p+}(0)$, as shown in Fig. 3(d). Such high transmission of $\Omega_{p+}$ can be understood as due to the strong ladder transparency created by the strong $\Omega_{d-}$ and the gain via the strong cross-talk that results from the absorption of $\Omega_{p-}$. The weak transmission of $\Omega_{p-}$ results from the net loss for $\Omega_{p-}$ due to $\chi^{(3)}$ assisted energy transfer to $\Omega_{p+}$. It was found that when the fields propagate farther into a longer medium ($\eta z > 6\gamma$), the transmission of the spectral wings of $\Omega_{p-}$ (at $\delta \sim \pm 2\gamma$) is reduced significantly.

## IV. EXPERIMENTAL RESULTS

In this section we demonstrate experimentally the control of cross-talk. The double-ladder system is realized experimentally using a cesium atomic vapor cell with the energy levels shown in Fig. 4(a). The probe laser is tuned near the $6^2S_{1/2}(j = 0, m_j = 0) \longrightarrow 6^2P_{3/2}(j = 1, m_j = \pm 1)$ D2 transition at a wavelength of 852.2 nm, and the drive laser is tuned near the $6^2P_{3/2}(j = 1, m_j = \pm 1) \longrightarrow 8^2S_{1/2}(j = 0, m_j = 0)$ transition at a wavelength of 794.3 nm. The natural linewidth $\gamma$ for the cesium D2 line is $\sim 2\pi \times 5.2$ MHz, and the natural linewidth $\Gamma$ of the transition between the states $6^2P_{3/2}$ and $8^2S_{1/2}$ is $\sim 2\pi \times 1.7$ MHz. The experimental setup is shown in Fig. 4(b). The 5-cm-long cesium vapor cell is installed inside a double-layer magnetic shield to eliminate the laboratory magnetic field. The density of the cesium vapor is controlled by the temperature of the cell. The transition of the drive field is driven by a single-frequency Ti:sapphire laser (Coherent 899, linewidth of ~500 kHz), and the laser beam is focused to a spot size of 500 $\mu$m. The probe transition is driven by an external-cavity diode laser (homemade ECDL, linewidth of ~1 MHz) that is focused to a spot size of 200 $\mu$m. In our experimental arrangement, the focus of the probe-beam waist is smaller than the drive; thus, the probe beam is present all the way inside the drive beam within the cell section. To maximize two-photon Doppler cancellation, the drive and probe beams are arranged in a counterpropagation configuration. The transmitted probe beam is separated from the drive beam using a 50:50 beam splitter, with a compensating half-wave plate to ensure that the polarization state is not disturbed by the Brewster angle from the beam splitter. To measure the transmitted spectra that correspond to the left- and right-circular polarized light, we employ two detectors and a quarter-wave plate that is oriented 45° to the polarization of the polarized beam splitter to form a balanced detection. The power of the probe and drive fields is controlled by adjusting the half-wave plate before the

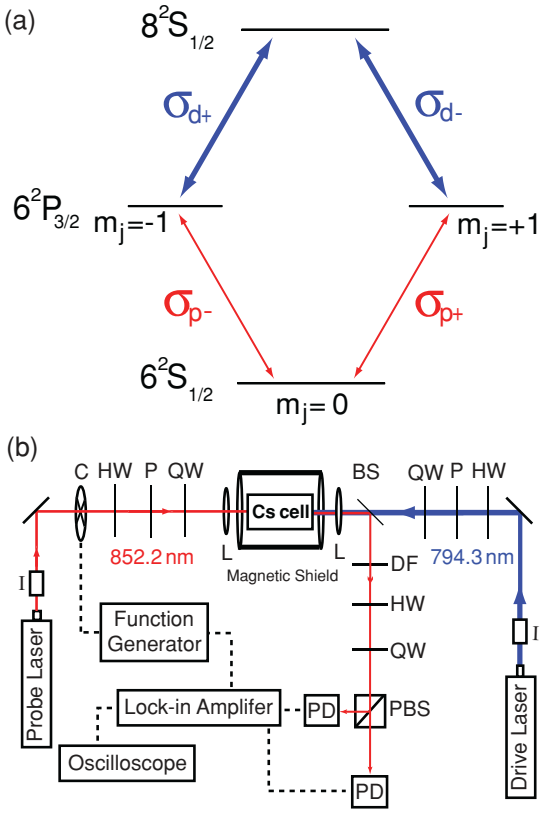


FIG. 4. (Color online) (a) Diagram showing the cesium atom energy levels. (b) Schematic diagram of the experimental setup: I, isolator; C, chopper; P, polarizer; HW, half-wave plate; QW, quarter-wave plate; PD, photodiode detector; L, focal lens; BS, beam splitter; PBS, polarized beam splitter; DF, dichroic filter.

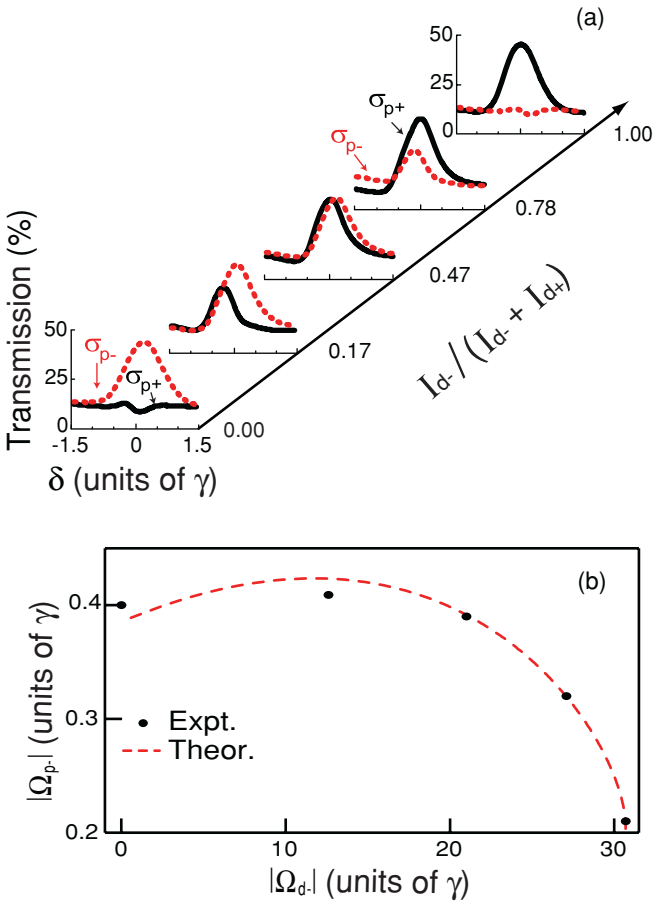


FIG. 5. (Color online) (a) The transmission of $\sigma_{p+}$ and $\sigma_{p-}$ probe fields is effectively controlled by the input intensity of the two control fields $\sigma_{d+}$ and $\sigma_{d-}$. The experimental parameters are: input linear probe with an intensity of $0.72\gamma^2$ ($|\Omega_{p+}|^2 = |\Omega_{p-}|^2 = 0.36\gamma^2$) and an elliptical drive field with a total intensity of $940\gamma^2$ ($|\Omega_{d-}|^2 + |\Omega_{d+}|^2 = 940\gamma^2$). The cesium atomic density in the cell is $N = 6 \times 10^{10}$ cm$^{-3}$. (b) Plot of maximum transmission power of probe $\sigma_{p-}$ field as a function of drive field $\sigma_{d-}$. The dashed curve is the theoretical calculation using Eq. (13). The parameters used for the theoretical fit are $\eta^{\text{eff}} = 0.003\eta$, $\Omega_{p\pm}^{\text{eff}} = 0.7\Omega_{p\pm}$, and $\Omega_{d\pm}^{\text{eff}} = 0.01\Omega_{d\pm}$. The chi-squared value of the fit for $|\Omega_{p-}|$ is 0.006. All laser-field intensities are presented in the form of Rabi frequencies squared, and all frequencies are scaled with $\gamma$.

polarizer, and the polarization of the probe and drive fields can be varied using a rotating polarizer and a quarter-wave plate. The probe transmission spectra that correspond to the left- and right-circular fields are recorded simultaneously by a digital oscilloscope.

In Fig. 5(a) we demonstrate that the transmission of the probe can be effectively controlled by an applied elliptically polarized drive field. Here, the drive fields are resonant with respect to their transitions, and the probe fields are tuned around resonance. In our experiment the input intensity of the linear probe is maintained at 6 mW/cm$^2$ $\sim 0.72\gamma^2$ ($|\Omega_{p+}|^2 = |\Omega_{p-}|^2 = 0.36\gamma^2$), and the total intensity of the elliptical drive field is maintained at $3 \times 10^4$ mW/cm$^2$ $\sim 940\gamma^2$ ($|\Omega_{d+}|^2 + |\Omega_{d-}|^2 = 940\gamma^2$). If only the drive $\sigma_{d+}$ and two probes $\sigma_{p+}$ and $\sigma_{p-}$ are present ($|\Omega_{d-}|^2 \sim 0$), then our system is composed of two distinct processes that drive the atomic dynamics—one with a standard ladder EIT for the $\sigma_{p-}$ transition and the other with a two-level system for the $\sigma_{p+}$ transition. Hence, the transmission of probe $\sigma_{p-}$ is maximum and that of $\sigma_{p+}$ is minimum. As the field strength of drive $\sigma_{d-}$ increases (note that the strength of $\sigma_{d+}$ field decreases simultaneously), both the spectral shape (i.e., linewidth and center frequency) and the intensity of the transmitted probe change. When the two drive fields are present with similar intensity, the transmissions of both of the probes reach maxima, and the spectra of the two probes are very similar—in agreement with the theoretical results shown in Fig. 2(c). The transmission of probe field $\sigma_{p-}$ at $\delta \sim 0$ as a function of the input drive field intensity of $\sigma_{d-}$ is shown in Fig. 5(b). The experimental results in this figure are in good agreement with the analytical solutions presented in Eq. (13).

In Ref. [9] the simple model for describing generation of a $\chi^{(3)}$ field via the resonant FWM process in the double-ladder system was used, where absorption of the generated field $\sigma_{p-}$ along the propagation direction and the cross-talk effect were ignored. In the present study, inclusion of both effects in the analytical calculation yields a finer and better quantitative agreement between the theoretical calculations and the experimental results as shown in Fig. 6.

To describe the experimental results [shown in Figs. 5(b) and Fig. 6] properly using the analytical solutions obtained, the effective Rabi frequency of probe $\Omega_{p\pm}$ and drive $\Omega_{d\pm}$ as well

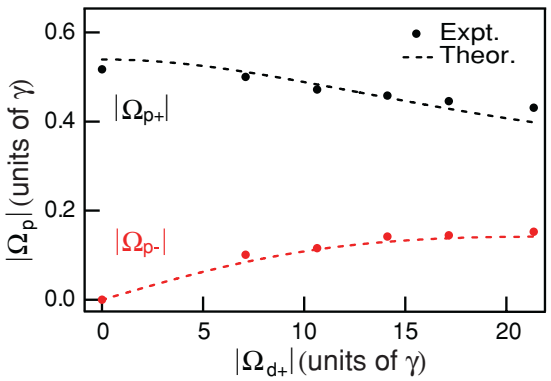


FIG. 6. (Color online) The transmission of the probe field $\sigma_{p+}$ and the generated field $\sigma_{p-}$ as a function of the input intensity of the drive $\sigma_{d+}$. All of the laser fields are on resonance with their respective transitions. Experimental parameters: $I_{p+} = 3$ mW/cm$^2$ ($|\Omega_{p+}(0)| = 0.6\gamma$), $I_{d+} = 1.5 \times 10^4$ mW/cm$^2$ ($|\Omega_{d-}| = 21\gamma$), and the cesium atomic density in the cell is $N = 3 \times 10^{10}$ cm$^{-3}$. The solid circles represent the experimental data, and the dashed curves represent the theoretical calculation using Eqs. (12) and (13). The parameters used for the theoretical fit are $\eta^{\text{eff}} = 0.006\eta$, $\Omega_{p\pm}^{\text{eff}} = 0.90\Omega_{p\pm}$, and $\Omega_{d\pm}^{\text{eff}} = 0.85\Omega_{d\pm}$. The chi-squared values of the fit for probe $|\Omega_{p+}|$ and the generated field $|\Omega_{p-}|$ are 0.0048 and 0.0056, respectively. All frequencies are scaled with $\gamma$.

as the effective optical depth $\eta$ were used. Thus, the coupling strength of the probe and drive transitions, the absorption of the drive field, and the atomic population distribution in the real atomic system of the cesium atom were taken into consideration. It was found that $\Omega_{d\pm}^{\text{eff}}$ becomes small in the optically dense medium because of the absorption of the drive fields. The small discrepancy between theory and experiment may be attributed to the complicated multiple-level structure of the cesium atom and line mixing due to the inhomogeneous broadening effect [28].

## V. SUMMARY

In summary, we have studied both theoretically and experimentally the propagation dynamics of two weak probes in a double-ladder system. We have demonstrated the explicit manifestation of the three-photon term in our analytical solutions for atomic polarization in the double-ladder system and also shown an interplay between $\chi^{(1)}$ and $\chi^{(3)}$ leading to the control of cross-talk. We have obtained analytical solutions for describing the dynamics of the probe field in the regimes where the contributions of $\chi^{(1)}$ and/or $\chi^{(3)}$ are significant and presented numerical results to demonstrate the controlled propagation dynamics of the cross-talk. We have also experimentally demonstrated control of the cross-talk and have shown that the analytical solutions presented yield good quantitative agreement with the experiment. Effective control of cross-talk in the double-ladder system could find many potential applications in optical communication [29] and in quantum information processing as a controllable correlated photon source [30].

## ACKNOWLEDGMENTS

The authors gratefully acknowledge useful discussions with Prof. G. S. Agarwal, Prof. Y. V. Rostovtsev, and Prof. M. O. Scully, and help with the experimental setup provided by Dr. L. Wang and Dr. J. Musser. Funding for this study was provided by the Air Force Research Laboratory (Contracts No. F33615-03-D-2329 and No. FA8650-09-C-200) and the Robert A. Welch Foundation (Grant No. A-1261).

[1] S. E. Harris, Phys. Today **50**, 36 (1997).
[2] S. E. Harris and L. V. Hau, Phys. Rev. Lett. **82**, 4611 (1999).
[3] M. M. Kash, V. A. Sautenkov, A. S. Zibrov, L. Hollberg, G. R. Welch, M. D. Lukin, Y. Rostovtsev, E. S. Fry, and M. O. Scully, Phys. Rev. Lett. **82**, 5229 (1999).
[4] See Secs. V and VI in, M. Fleischhauer, A. Imamoglu, and J. P. Marangos, Rev. Mod. Phys. **77**, 633 (2005).
[5] M. Xiao, Y. Q. Li, S. Z. Jin, and J. Gea-Banacloche, Phys. Rev. Lett. **74**, 666 (1995); J. Gea-Banacloche, Y. Q. Li, S. Z. Jin, and M. Xiao, Phys. Rev. A **51**, 576 (1995).
[6] Y. Zhang, A. W. Brown, and M. Xiao, Phys. Rev. A **74**, 053813 (2006).
[7] S. Li, X. Yang, X. Cao, C. Zhang, C. Xie, and H. Wang, Phys. Rev. Lett. **101**, 073602 (2008).
[8] P. S. Hsu, A. K. Patnaik, and G. R. Welch, J. Mod. Opt. **55**, 3109 (2008).
[9] P. S. Hsu, A. K. Patnaik, and G. R. Welch, Opt. Lett. **33**, 381 (2008).
[10] A. S. Zibrov, M. D. Lukin, L. Hollberg, and M. O. Scully, Phys. Rev. A **65**, 051801(R) (2002).
[11] J. T. Schultz, S. Abend, D. Döring, J. E. Debs, P. A. Altin, J. D. White, N. P. Robins, and J. D. Close, Opt. Lett. **34**, 2321 (2009).
[12] A. M. Akulshin, R. J. McLean, A. I. Sidorov, and P. Hannaford, Opt. Express **17**, 22861 (2009).
[13] F. E. Becerra, R. T. Willis, S. L. Rolston, and L. A. Orozco, Phys. Rev. A **78**, 013834 (2008).
[14] R. T. Willis, F. E. Becerra, L. A. Orozco, and S. L. Rolston, Phys. Rev. A **79**, 033814 (2009).
[15] S. Wielandy and A. L. Gaeta, Phys. Rev. Lett. **81**, 3359 (1998).
[16] A. K. Patnaik and G. S. Agarwal, Opt. Commn. **179**, 97 (2000).
[17] A. K. Patnaik and G. S. Agarwal, Opt. Commn. **199**, 127 (2001).
[18] T. H. Yoon, C. Y. Park, and S. J. Park, Phys. Rev. A **70**, 061803(R) (2004).
[19] S. J. Park, C. Y. Park, and T. H. Yoon, Phys. Rev. A **71**, 063819 (2005).
[20] D. Cho, J. M. Choi, J. M. Kim, and Q-Han Park, Phys. Rev. A **72**, 023821 (2005).
[21] K. Pandey, A. Wasan, and V. Natarajan, J. Phys. B **41**, 225503 (2008).
[22] G. Morigi, S. Franke-Arnold, and G. L. Oppo, Phys. Rev. A **66**, 053409 (2002).

[23] S. Kajari-Schröder, G. Morigi, S. Franke-Arnold, and G. L. Oppo, Phys. Rev. A **75**, 013816 (2007).
[24] E. A. Korsunsky, N. Leinfellner, A. Huss, S. Baluschev, and L. Windholz, Phys. Rev. A **59**, 2302 (1999).
[25] A. F. Huss, E. A. Korsunsky, and L. Windholz, J. Mod. Opt. **49**, 141 (2002).
[26] S. Menon and G. S. Agarwal, Phys. Rev. A **59**, 740 (1999).
[27] M. O. Scully and M. S. Zubairy, *Quantum Optics* (Cambridge University Press, Cambridge, UK, 1997).
[28] W. Demtröder, *Laser Spectroscopy* (Springer, Berlin, 1998).
[29] R. W. Boyd, D. J. Gauthier, and A. L. Gaeta, Opt. Photon. News **17**, 18 (2006).
[30] A. K. Patnaik, G. S. Agarwal, C. H. Raymond Ooi, and M. O. Scully, Phys. Rev. A **72**, 043811 (2005).